Photorefractivity in polymer-stabilized nematic liquid crystals

Gary P. Wiederrecht[a] and Michael R. Wasielewski[a,b]

[a]Chemistry Division, Argonne National Laboratory, Argonne, IL 60439-4831
[b]Department of Chemistry, Northwestern University, Evanston, IL 60208-3113

ABSTRACT

Polymer-stabilized liquid crystals, consisting of low concentrations of a polymeric electron acceptor, are shown to exhibit significantly enhanced photorefractive properties. The charge generation and transport properties of these composite systems are strongly modified from nematic liquid crystals doped with electron donors and acceptors. The new composites are produced by polymerizing a small quantity of a 1,4:5,8-naphthalenediimide electron acceptor functionalized with an acrylate group in an aligned nematic liquid crystal. Photopolymerization creates an anisotropic gel-like medium in which the liquid crystal is free to reorient in the presence of a space charge field, while maintaining charge trapping sites in the polymerized regions of the material. The presence of these trapping sites results in the observation of longer lived, higher resolution holographic gratings in the polymer-stabilized liquid crystals than observed in nematic liquid crystals alone. These gratings display Bragg regime diffraction. Asymmetric beam coupling, photo-conductivity, and four-wave mixing experiments are performed to characterize the photophysics of these novel materials.

Keywords: Photorefractive Materials; Polymer-Stabilized Liquid Crystals; Non-Linear Optics; Photoconductivity

1. INTRODUCTION

Photorefractive materials hold great promise for optical device applications in the areas of reversible optical holography, noise-free optical image amplification, phase conjugate mirrors, and other optical signal processing techniques.[1-3] The photorefractive effect is a light-induced change in the refractive index of a nonlinear optical material. It results from the creation of an electric field induced by directional charge transport over macroscopic distances. If the material is electro-optic, the electric (or space charge) field can then modulate the refractive index of the material. When the effect is properly optimized, an image can be stored and retrieved with no loss of optical fidelity using phase conjugation techniques.

Research on the photorefractive effect has blossomed over the past several years. As a consequence of the outstanding optical quality and commercial availability of inorganic ferroelectric materials such as barium titanate and lithium niobate, photorefractive holographic data storage systems have been designed and developed to the point that commercialization of these systems is now being attempted.[4] Although these materials perform well, the availability of materials that are useful over a wide range of wavelengths and have significantly lower cost would dramatically enhance the versatility of the photorefractive effect. In this pursuit, the 1990's have seen the advent of photorefractive polymers and liquid crystals.[5-17] These materials have many attractive properties, such as low dielectric constants, which minimize dielectric shielding of the space charge field, low cost, and relatively simple syntheses. However, the development of useful organic materials is challenging because the photorefractive effect requires the simultaneous optimization of electro-optic properties, charge generation efficiency, charge transport over macroscopic distances, and charge trapping. Nonetheless, organic materials have been developed to the point that their photorefractive gains are now larger than those exhibited by their inorganic counterparts.

One of the reasons for the large photorefractive gains in organic materials is the development of low glass transition temperature polymers that permit orientational motion of the nonlinear optical chromophores within the space-charge field. This provides a birefringence contribution to the index of refraction change of the photorefractive grating over and above that of the electro-optic effect. In fact, recent studies have shown that a large fraction of the photorefractive gain in the

DISCLAIMER

highest gain polymers reported to date is due to orientational responses.[7] In light of these results, several groups have recently explored nematic liquid crystals for photorefractive effects.[10-15,17,18] Nematic liquid crystals have long been known to reorient in much lower electric fields, even reorienting in optical fields. Thus, the space charge fields that are required to produce comparable changes in the refractive index in nematic liquid crystals are orders of magnitude lower than for polymeric materials. Space charge fields that induce large photorefractive effects in nematic liquid crystals are on the order of 10V/cm, compared to the 500,000 V/cm or higher cited for polymeric materials.

The disadvantages of low molar mass liquid crystals as photorefractive media are 1)the large fringe spacings generally required to induce the effect do not permit for Bragg regime diffraction and 2) the general lack of long-lived gratings. Given these limitations, several groups have recently reported efforts using either polymer-dispersed liquid crystals or polymer-stabilized liquid crystals (PSLCs).[16,19,20] Polymer-dispersed liquid crystals have a high concentration of polymer, so that phase separation produces droplets within the material. Alignment of the liquid crystal droplet directors with an applied electric field produces a transparent sample. Polymer-stabilized liquid crystals consist of only 1-2% of a polymeric material that creates an anisotropic, transparent, gel-like material. Both of these materials alter the charge transport characteristics of the liquid crystals from purely ion diffusion to include migration of charge through conductive polymers and/or charge trapping in the polymer. These experiments have proven successful for creating both longer lived gratings and Bragg regime diffraction. We report here our efforts for creating polymer-stabilized liquid crystals for photorefractive applications.

2. EXPERIMENTAL METHODS

In order for PSLCs to exhibit photorefractivity, they must be photoconductive so that a space-charge field can be generated. Therefore, easily oxidized and reduced dopants must be added for efficient photoinduced charge generation and charge migration over bulk distances. With this in mind, the building blocks that make up our PSLCs are shown in Figure 1. The liquid crystal itself is a eutectic liquid crystal mixture of 35% (weight %) 4'-(*n*-octyloxy)-4-cyanobiphenyl (8OCB) and 65% 4'-(n-pentyl)-4-cyanobiphenyl (5CB). The liquid crystal is then doped with the chromophore perylene ($2x10^{-3}$M), which has a broad absorption band that peaks at 443 nm and permits the use of the 514 nm line of an Ar^+ beam. Perylene is also easily oxidized, with a one-electron oxidation potential of 0.8 eV vs. a saturated calomel electrode. The sample is then doped with 2% (mol %) of NIAC, an acrylate monomer containing an easily reduced naphthalene diimide moiety (-0.5 eV vs. the saturated calomel electrode). The synthesis of NIAC is described elsewhere.[20] Finally, 0.5 % (mol %) of benzoin methyl ether (BME) is added to function as a photoinitiator.

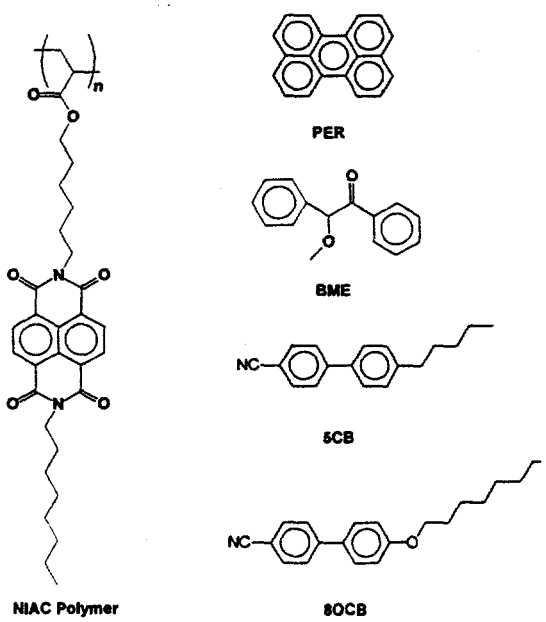

Figure 1. Components of the photorefractive polymer-stabilized liquid cyrstal.

The samples were prepared as follows. Indium-tin-oxide (ITO) coated glass slides were treated with the surfactant octadecyltrichlorosilane to induce LC director alignment perpendicular to the plane of the glass slides (homeotropic alignment).[21] Teflon spacers were used to create 26 μm thick optical cells. The LC was drawn into the cell through capillary action, and alignment occurred in approximately 30 min. Photopolymerization of the acrylate monomers was performed within the aligned LC samples with 365 nm light at an intensity of 2 mW/cm^2. Polymerization times of 1, 2, 4, and 6 minutes were utilized. The polymerized samples appeared slightly more hazy and pressure applied to the cell did not misalign the material as with the unpolymerized samples.

The geometry of the experiment is illustrated in Figure 2. Two coherent, 2.5 mW, 514-nm beams from a continuous wave Ar^+ laser were overlapped in the sample. The beams were unfocused and had a 1/*e* diameter at the sample of 2.5 μm. Voltages of up to 2 volts were applied to the polymerized samples, producing applied electric fields up to 800 V/cm. For

those experiments performed in the thin grating regime, beam coupling manifested itself as an increase in the intensity of all of the diffracted and undiffracted light from one beam and a corresponding drop in the intensity of the other beam and its diffracted beams.

Other phenomena in liquid crystals can lead to the observation of asymmetric beam coupling in the thin grating regime, including thermal, photochromic, order-disorder, and phase change effects.[18,22] However, these possibilities can be ruled out through diagnostic experiments that are discussed in the literature.[11,18] First, the effect is not observed unless a static electric field is present, suggesting that a static internal field, such as a space charge field, is present that leads to director axis reorientation. No effect is observed for an ac applied electric field. Second, the sample must be tilted relative the writing beams' bisector, as shown in Fig. 2, in order to see the effects. This indicates that a component of the grating wavevector must lie along the direction of the applied electric field in order for directional charge transport to occur along the wavevector. Third, a grating is only observed when the grating wavevector and the polarization of the laser light lie in the same direction, indicating that the index change is a result of reorientation of the liquid crystal molecules in the plane of the two writing beams.[11,18] None of the previously observed alternative effects can be explained by these observations.

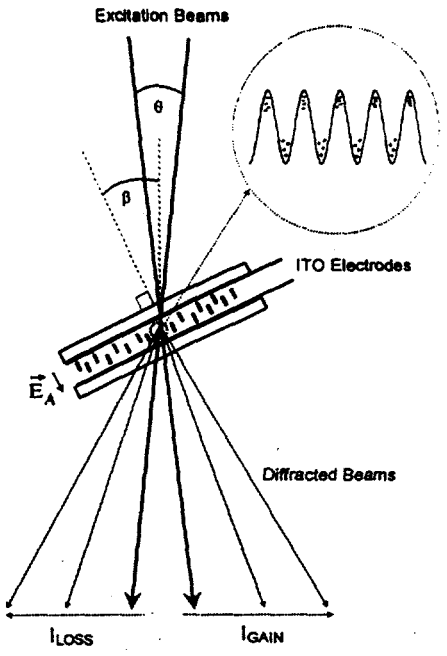

Figure 2

In addition to these observations, we have also performed a variety of conductivity experiments that are consistent with the photorefractive mechanism. We have performed dark conductivity and photoconductivity measurements and have shown that increases in photoconductivity produce larger photorefractive effects.[12,13] We also measured the diffusion constant values for the anions and cations.[13] We showed conclusively that the greater the difference between these two values, the larger our photorefractive response. This is consistent with the creation of a larger space charge field as indicated by:

$$E_{sc} = \frac{-k_B T q}{2e_o} \frac{D^+ - D^-}{D^+ + D^-} \frac{\sigma_{ph}}{\sigma_{ph} + \sigma_d} \sin qx \qquad (1)$$

Here, σ_{ph} is the photoconductivity, σ_d is the dark conductivity, k_B is the Boltzmann constant, e_o is the charge of a proton, q is the wavevector of the grating, and D^+ and D^- are the diffusion constants for the cations and anions, respectively. It is clear that the two factors which determine the magnitude of the space charge field are the difference in the photoconductivity versus dark conductivity and the difference in the diffusion coefficients of the cations and anions. These factors allow for one set of charges to trap in the illuminated regions of the interference pattern and for the opposing charges to migrate into the nulls of the interference pattern before trapping.

Four-wave mixing and photoconductivity measurements were also performed to characterize the samples. For the four wave mixing experiments, a third p-polarized HeNe beam was arranged in boxcar pattern, and the diffracted HeNe beam that constituted the fourth "corner" of the box was monitored for time resolved signal. For the photoconductivity experiments, a Keithley model 485 picoammeter was used. Although the photocurrent is relatively low (~10^{-9} A) for incident CW powers of 100 mW/cm^2, the 10MΩ resistance of the samples provided for reproducible results. Both experiments were digitized using a National Instruments AT-MIO-16 A/D board in conjunction with LabWindows/CVI software.

3. RESULTS

The improved photorefractive grating resolution due to polymer stabilization is illustrated by the asymmetric beam coupling measurements shown in Figure 3. The unpolymerized samples do not show any measurable beam coupling for fringe spacings (Λ) below 8 μm, whereas the polymerized samples exhibit beam coupling down to Λ=2.5 μm. We found that the samples polymerized for 2 minutes exhibited the highest beam coupling ratios at small fringe spacings. Samples that were polymerized for longer times exhibited reduced beam coupling at all fringe spacings, whereas those polymerized for

only 1 minute showed high beam coupling at larger fringe spacings, but no beam coupling at shorter fringe spacings in a manner similar to the unpolymerized samples. The dependence of two-beam coupling on polymerization time suggests that optimal photorefractivity is observed when polymerization of NIAC is not quantitative, and that unpolymerized monomers are present along with longer chains of polymerized NIAC. The incomplete polymerization permits mobile PER cations and monomeric NIAC anions that provide for bulk charge transport to co-exist with the less mobile polymerized NIAC electron acceptor trapping sites. Figure 4 shows the kinetics of beam coupling at Λ=4.8 μm for samples that were polymerized for 2 minutes. The inset to Figure 4 shows the beam coupling at the smallest fringe spacing of 2.5 μm.

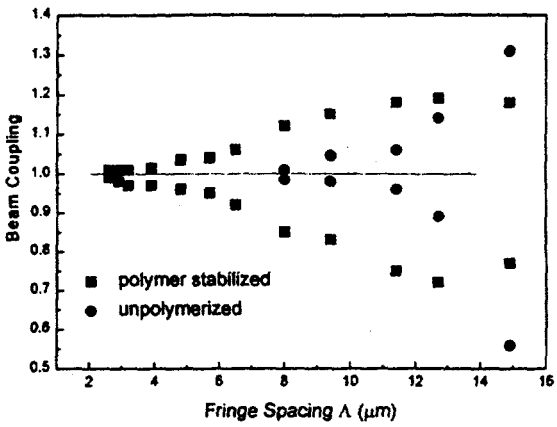

Figure 3. The improved resolution of the photorefractive gratings in polymer stabilized liquid crystals is illustrated.

We also used different electron acceptors to probe the optimal free energy for charge separation in the PSLC environment. Marcus theory predicts that the rate of charge separation (k_{CS}) will be the greatest when the exothermicity of the reaction is equal to the sum of the reorganization energy of the solvent (λ_o) and the internal vibrational reorganization energy of the ions (λ_i).[23-25] For free energies of charge separation (ΔG_{CS}) that are more or less than the total reorganization energy, the rates of charge separation will be slower. This can be restated by the equations:

$$k_{CS} = \left(\frac{2\pi}{\hbar}\right) V_{DA}^2 \left(\frac{1}{4\pi\lambda RT}\right)^{1/2} \exp\left(-(\Delta G_{CS} + \lambda)^2 / 4\lambda RT\right) \qquad (2)$$

$$\Delta G_{CS} = E_{OX} - E_{RED} - E_S \qquad (3)$$

where $\lambda = \lambda_o + \lambda_i$. Here, V_{DA} is the electronic coupling matrix element between the donor and acceptor, E_{OX} is the oxidation potential of PER, and E_{RED} is the reduction potential for the electron acceptor. The excited state energy (E_s) for *PER is 2.8 eV, so that the free energy driving force for the generation of solvent separated ions is 1.5 eV.[13,24] Following previous precedent, these values ignore the Coulomb term which is small in polar environments.[24] Although the optimal ΔG_{CS} value at first glance appears to be rather high, it has been established that the solvent reorganization energies for solvent separated ion pairs, as opposed to tight ion pairs, are higher.[24] In addition to optimizing ΔG_{CS}, the value for ΔG_{CR} (charge return) is placed in the Marcus inverted regime, resulting in slower rates for charge return and therefore increasing the efficiency of mobile charge generation.[24] We expect that the optimal free energies for charge separation in a PSLC will be higher than that for purely nematic materials because the initial ion pair will be destabilized in the more viscous environment. In order to test this hypothesis, we also tried functionalizing a pyromellitimide electron acceptor with the acrylate (PIAC) to use as the polymer in the PSLC. The reduction potential of PIAC is 0.3 V higher than NIAC, resulting in a lower driving force for charge separation with the PIAC system. The photorefractive response of the PIAC system was lower than that for the NIAC system, indicating lower efficiency of the charge separation reaction. Given that the

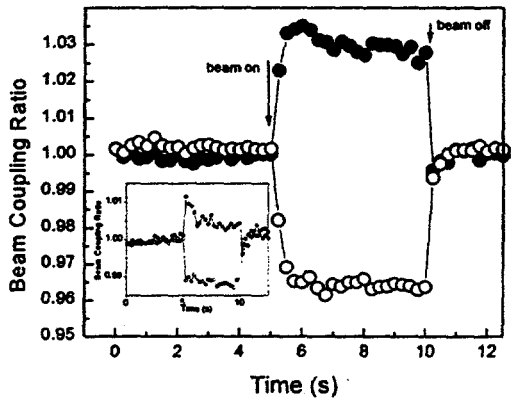

Figure 4. The kinetics of asymmetric beam coupling within the PSLC is shown for Λ=4.8 μm. The inset shows the beam coupling kinetics for Λ=2.5 μm.

a)

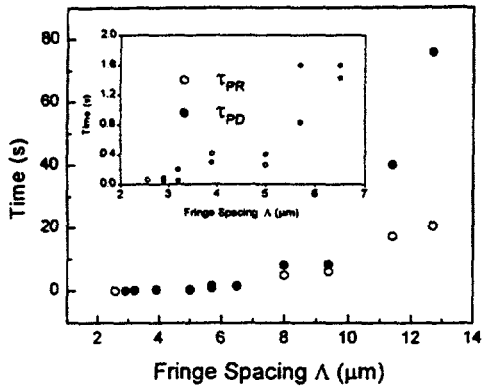

b)

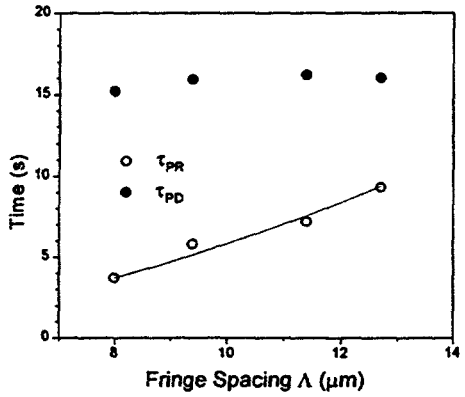

Figure 5. The rise, τ_{PR} and decay times τ_{PD} of the photorefractive grating vs Λ are illustrated for the (a) PSLC and the (b) unpolymerized LC. The inset in (a) is a blowup of the smallest fringe spacings studied. The unpolymerized LC decay times exhibit a quadratic dependence on fringe spacing, consistent with a ion diffusion, whereas the PSLCs show a steeper dependence vs. Λ.

pyromellitimide acceptor/PER combination has been found to be optimal for pure nematic liquid crystals, the increased driving force requirements of the PSLCs is evident.[13]

The photorefractive rise (τ_{pr}) and decay (τ_{pd}) times vs. Λ, as measured by the four wave mixing experiments, are shown in Figures 5a and 5b for the polymerized and unpolymerized samples, respectively. The decay times are measured following the blockage of either one of the writing beams. Note that the rise times of the photorefractive gratings in the polymerized samples are always faster than the decay times when one beam is blocked for all but the smallest three fringe spacings. Conversely, for the unpolymerized samples, the decay times are always faster than the rise times even for the large fringe spacings studied. Therefore, the polymerized samples clearly produce a more stable photorefractive grating and, as a result, smaller fringe spacings can be attained.

The time-resolved photoconductivity measurements shown in Figure 6 give further support for a difference in

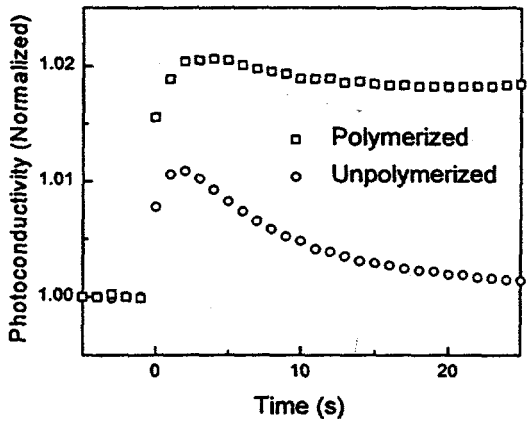

Figure 6. The improved photoconductivity of the PSLC relative to the LC is illustrated.

photoinduced charge transport in the polymerized samples vs the unpolymerized samples. For an incident laser power of 100 mW/cm^2 and a spot size of 2.5 mm, the decay time of the photoconductivity for the unpolymerized samples is 7.4 s, whereas the photoconductivity of the polymerized samples does not significantly drop over a 30 s period. Also, the photoconductivity of the polymerized sample is nearly twice that of the unpolymerized samples even at the peak of the unpolymerized photoconductive response. The unnormalized values for the dark conductivity in both samples is 1.7×10^{-10} S cm^{-1}. The photoconductivity is 5.8×10^{-11} S cm^{-1} for the unpolymerized sample and 1.1×10^{-10} S cm^{-1} for the PSLC at an optical intensity of 2 W cm^{-2}.

4. DISCUSSION

In order to determine whether the grating is a thin (Raman-Nath) or volume (Bragg) grating, the following well known parameter can be used: [26]

$$Q = \frac{2\pi D\lambda}{\Lambda^2 n} \qquad (4)$$

where λ is the wavelength of the light, n is the index of refraction, and D is the thickness of the grating ($D=d/\cos\beta$, where d is the cell thickness). For $Q<<1$, the grating is considered to be a plane grating, and for $Q>>1$, a volume grating is created. Although the literature does not appear to specifically designate an exact value for Q in which the thick grating regime is reached, the most rigorous treatments suggest that Q values of 10 are required to produce a true volume hologram [27]. For our samples, Q=10 is achieved for Λ=2.6 μm, when D=26 μm/cos 30° = 30 μm, and n=1.5. At this fringe spacing, our samples still exhibit a small amount of beam coupling (about ±1%), so the PSLCs can be considered to be operative in the thick grating regime. This compares favorably to the best case scenario exhibited by the LCs with no polymer stabilization, where beam coupling is observed for fringe spacings no smaller than Λ=8 μm, giving Q = 1.

Given that the samples operate in the nominally thick grating regime, the net photorefractive gain (Γ) can be calculated assuming an exponential dependence on the thickness of the sample:[5]

$$\Gamma = \frac{1}{D}\cdot\left[\ln\frac{I_{12}}{I_1} - \ln\left(2 - \frac{I_{12}}{I_1}\right)\right] - \alpha \qquad (5)$$

where α is the sample absorbance, I_1 is the intensity of beam 1 in the absence of beam 2, and I_{12} is the intensity of beam 1 with beam 2 applied. The absorbance of the sample at 514 nm is 0.003, resulting in values for α of only 1 cm^{-1}. Therefore, for Λ = 2.5 μm a net photorefractive gain of Γ = 5 cm^{-1} results. For somewhat less rigorous treatments of the Q value, higher photorefractive gains are calculated. For example, some researchers suggest that the condition $\Lambda^2 \approx D\lambda$ is sufficient for the thick grating regime to be reached, so that for Λ = 4 μm (Q=4) beam coupling of ± 3% is observed and the net photorefractive gain is 15 cm^{-1}.[16]

The beam coupling, four-wave mixing, and photoconductivity data indicate that the mechanism for charge transport within the PSLCs differs from that within the unpolymerized samples. Further support for ion diffusion as the mechanism for photorefractivity in the unpolymerized samples is the quadratic dependence of the grating decay time vs. fringe spacing, as shown in Figure 5b. [18,26] However, the data for the polymerized samples clearly indicate a decay time dependence vs. Λ that is far greater than quadratic. Given these facts, the photorefractive data from the polymerized samples can be explained in terms of a model in which the polymerized NIAC electron acceptor functions as an electron trap site. The existence of less mobile electron traps can explain the smaller fringe spacings at which asymmetric two beam coupling is observed. Since Debye diffusion lengths are proportional to $D^{1/2}$, the drop in the best value of Λ from 8 μm for the unpolymerized samples to 2.5 μm for the PSLCs indicates that the polymerized NIAC functions as an electron trap with an average diffusion constant that is approximately one order of magnitude smaller than that of monomeric $NIAC^-$. In this model, it is critical that the polymerization is not quantitative so that mobile monomers of $NIAC^-$ are present to carry out charge transport between the fringes of the optical interference pattern.

At the same time, the polymerized NIAC may play a role in improving the photoconductivity of the PSLCs, as reported above and illustrated in Figure 6. Improvements in the photoconductivity are due to either an increase in the quantum efficiency of mobile charge generation (ϕ) or an increase in the mobility of the ions (μ) because $\sigma_{ph} \propto \phi\mu$[28]. If we assume that the acrylate chain on the monomeric NIAC acceptor does not significantly alter the mobility of the reduced NIAC monomer relative to the corresponding *N,N*-di-n-octyl derivative previously examined,[12] the quantum efficiency of charge generation must improve. Collisions of PER* with NIAC create PER^+-$NIAC^-$ ion pairs, and a fraction of the population of these initial ion pairs form the solvent-separated ions necessary for bulk charge transport. If the initial PER^+-$NIAC^-$ ion pair is formed on a polymerized NIAC strand, there is a greatly increased probability that charge hopping will occur to other NIAC molecules on the same polymer strand. Thus, an additional mechanism for creating solvent separated ions is present in the PSLCs that is not present in conventional LCs.

Another significant difference between the PSLCs and LCs is the behavior of the decay of the photorefractive gratings with both beams blocked compared to one beam blocked. The photorefractive grating decays very quickly for the PSLCs when both writing beams are blocked, whereas slower grating decay is observed when only one beam is blocked, as

measured by four-wave mixing experiments shown in Figure 7. In fact, the lifetimes of the gratings are enhanced by more than an order of magnitude when one beam is incident on the sample. No such lifetime increase is observed for photorefractive gratings in unpolymerized LCs, illustrated by the inset to Fig. 7. These experiments show that a photoinduced process occurs in the PSLCs that promotes charge separation and inhibits charge recombination.

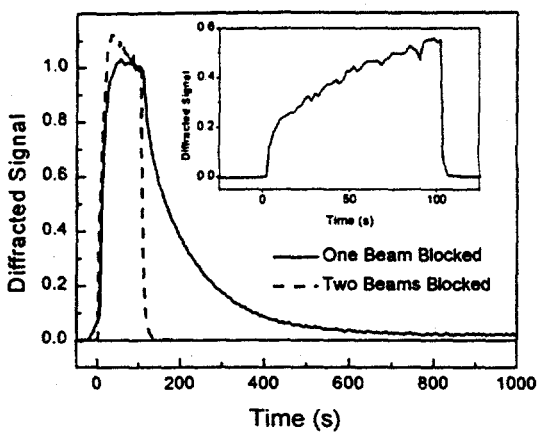

Figure 7. The difference in decay kinetics for one beam blocked vs two beams blocked in the PSLC is illustrated. The lifetime of the grating is enhanced when one beam is incident on the sample. The inset shows the decay kinetics for the unpolymerized LC when one beam is incident on the sample. No enhancement of the grating lifetime is observed. Both beams are incident on the sample at t = 0, and either one or both beams are blocked as specified above at t = 100 s.

One possible explanation for these observations is suggested by focusing on the electron transfer equilibrium that occurs between monomeric NIAC$^-$ and the polymerized NIAC traps. After the grating is formed, removal of both laser beams from the sample results in rapid charge recombination between monomeric NIAC$^-$ and PER$^+$ because of the greater mobility of monomeric NIAC$^-$ relative to that of polymerized NIAC$^-$. The rapid depletion of monomeric NIAC$^-$ in the PSLCs results in a shift in the charge equilibrium between monomeric NIAC and polymerized NIAC$^-$ to move charge onto the more mobile monomeric NIAC, which in turn transfers the electron back to PER$^+$. This process most likely occurs in parallel with direct electron transfer from polymerized NIAC$^-$ to PER$^+$. On the other hand, when a single laser beam remains incident on the grating, PER$^+$ and NIAC$^-$ are generated throughout the existing grating. This laser beam generates excess NIAC$^-$ which shifts the equilibrium for electron transfer between monomeric NIAC and polymerized NIAC$^-$ to favor retention of charge on polymerized NIAC. Thus, the previously generated spatial grating due to electron trapping on polymerized NIAC is preserved for a longer period of time.

5. CONCLUSIONS

We have shown that PSLCs are capable of forming photorefractive gratings that operate in the thick grating (Bragg) regime. Polymer stabilization alters the charge transport and trapping characteristics of LCs, resulting in longer lived gratings, while maintaining the advantages of high orientational birefringence within LCs. Furthermore, very low applied electric fields (800 V/cm) and low optical intensities (100 mW/cm^2) are required to create large photorefractive effects in these materials. It is expected that further optimization of the photophysical and redox potentials of the donor-acceptor additives and of their incorporation into the polymer structure within the PSLCs will continue to improve the photorefractive performance of these materials.

6. ACKNOWLEDGMENTS

We gratefully acknowledge support from the Office of Computational and Technology Research, Division of Advanced Energy Projects and Technology Research, U.S. Department of Energy, under contract W-31-109-ENG-38.

7. REFERENCES

1. J. Feinberg "Photorefractive Nonlinear Optics", *Physics Today* **October**, pp. 46-52, 1988.
2. C. R. Giuliano "Applications of Optical Phase Conjugation", *Physics Today* **April**, pp. 27-35, 1981.
3. P. Gunter; J. P. Huignard *Photorefractive Materials and Their Applications 1: Fundamental Phenomena*; Springer-Verlag: Berlin, 1988.
4. D. Psaltis; F. Mok "Holographic Memories", *Scientific American* **November**, pp. 70, 1995.
5. W. E. Moerner; S. M. Silence "Polymeric Photorefractive Materials", *Chem. Rev.* **94**, pp. 127-155, 1994.

6. Y. Zhang; Y. Cui; P. N. Prasad "Observation of Photorefractivity in a Fullerene-Doped Polymer Composite", *Phys. Rev. B* **46**, pp. 9900, 1992.
7. B. L. Volodin; B. Kippelen; K. Meerholz; B. Javidi; N. Peyghambarian "A Polymeric Optical Pattern Recognition System for Security Verification", *Nature* **383**, pp. 58-60, 1996.
8. S. Ducharme; J. C. Scott; R. J. Twieg; W. E. Moerner "Observation of the Photorefractive Effect in a Polymer", *Phys. Rev. Lett.* **66**, pp. 1846-1849, 1991.
9. L. Yu; W. K. Chan; A. Peng; A. Gharavi "Multifunctional Polymers Exhibiting Photorefractive Effects", *Acc. Chem. Res.* **29**, pp. 13-21, 1996.
10. I. C. Khoo; H. Li; Y. Liang "Observation of Orientational Photorefractive Effects in Nematic Liquid Crystals", *Opt. Lett.* **19**, pp. 1723-25, 1994.
11. E. V. Rudenko; A. V. Sukhov "Photoinduced Electrical Conductivity and Photorefraction in a Nematic Liquid Crystal", *JETP Lett.* **59**, pp. 142-46, 1994.
12. G. P. Wiederrecht; B. A. Yoon; M. R. Wasielewski "High Photorefractive Gain in Nematic Liquid Crystals Doped with Electron Donor and Electron Acceptor Molecules", *Science* **270**, pp. 1794-97, 1995.
13. G. P. Wiederrecht; B. A. Yoon; M. R. Wasielewski "Photorefractive Liquid Crystals", *Adv. Mat.* **8**, pp. 535-39, 1996.
14. G. P. Wiederrecht; B. A. Yoon; M. R. Wasielewski "Photorefractive Liquid Crystals Doped with Electron Donor and Acceptor Molecules", *Synth. Met.* **84**, pp. 901-2, 1997.
15. G. P. Wiederrecht; B. A. Yoon; W. A. Svec; M. R. Wasielewski "Photorefractivity in Nematic liquid Crystals Containing Electron Donor-Acceptor Molecules that Undergo Intrmolecular Charge Separation", *J. Am. Chem. Soc.* **119**, pp. 3358, 1997.
16. H. Ono "Orientational photorefractive effects observed in polymer-dispersed liquid crystals", *Opt. Lett.* **22**, pp. 1144-46, 1997.
17. H. Ono; I. Saito; N. Kawatsuki "Photorefractive Bragg diffraction in high- and low-molar-mass liquid crystal mixtures", *Appl. Phys. Lett.* **72**, pp. 1942-44, 1998.
18. I. C. Khoo "Orientational Photorefractive Effects in Nematic Liquid Crystal Films", *IEEE J. Quant. Elec.* **32**, pp. 525-534, 1996.
19. A. Golemme; B. L. Volodin; B. Kippelen; N. Peyghambarian "Photorefractive polymer-dispersed liquid crystals", *Opt. Lett.* **22**, pp. 1226-28, 1997.
20. G. P. Wiederrecht; M. R. Wasielewski "Photorefractivity in Polymer-Stabilized Nematic Liquid Crystals", *J. Am. Chem. Soc.* **120**, pp. 3231-3236, 1998.
21. I. C. Khoo *Liquid Crystals: Physical Properties and Nonlinear Optical Phenomena*; Wiley: New York, 1995.
22. I. C. Khoo "Holographic Grating Formation in Dye- and Fullerene C60-doped Nematic Liquid-Crystal Film", *Opt. Lett.* **20**, pp. 2137-39, 1995.
23. R. A. Marcus "On the Theory of Oxidation-Reduction Reactions Involving Electron Transfer. I.", *J. Chem. Phys.* **24**, pp. 966, 1956.
24. I. R. Gould; D. Ege; J. E. Moser; S. Farid "Efficiencies of Photoinduced Electron-Transfer Reactions: Role of the Marcus Inverted Region in Return Electron Transfer within Geminate Radical-Ion Pairs", *J. Am. Chem. Soc.* **112**, pp. 4290-4301, 1990.
25. M. R. Wasielewski "Photoinduced Electron Transfer in Supramolecular Systems for Artificial Photosynthesis", *Chem. Rev.* **92**, pp. 435-461, 1992.
26. H. J. Eichler; P. Gunter; D. W. Pohl *Laser-Induced Dynamic Gratings*; Springer-Verlag: Berlin, 1986.
27. Y. H. Ja "Degenerate Four-Wave Mixing Experiments in Bi12GeO20 Crystals", *Elect. Lett.* **17**, pp. 488-9, 1981.
28. J. C. Scott; L. T. Pautmeier; W. E. Moerner "Photoconductivity Studies of Photorefractive Polymers", *J. Opt. Soc. Am. B* **9**, pp. 2059-64, 1992.